

# Kinetic Aspects of Nonlinear Effects in Asymmetric Catalysis

DONNA G. BLACKMOND\*

Department of Chemistry, University of Hull,  
Hull HU6 7RX, United Kingdom

Received October 28, 1999

## ABSTRACT

Probing catalyst systems for a nonlinear relationship between product enantioselectivity and catalyst enantiopurity is now commonly being used as a mechanistic tool. We show that in some cases striking consequences for reaction rate can ensue for reactions carried out using non-enantiopure catalysts. We also demonstrate how consideration of the kinetic behavior may serve to enhance the use of nonlinear effects as a diagnostic tool for identifying active catalytic species and for providing mechanistic insight. Kinetic information may also help in the development of efficient synthetic strategies using non-enantiopure systems.

## Introduction

Over the past decade, an increasing number of reports have appeared describing asymmetric catalytic reactions where the product enantioselectivity is not proportional to the enantiomeric excess of the chiral ligand employed. Such nonlinear effects can be traced to earlier observations of unusual physical and chemical properties sometimes exhibited by mixtures of enantiomers in solution, attributed to the formation of diastereomeric species or higher order agglomerates.<sup>1–3</sup> Wynberg and Feringa recognized that this nonideal behavior may also have implications when a chemical reaction occurs in a non-enantiopure mixture.<sup>4</sup> This was first quantified by Kagan and co-workers<sup>5</sup> both with theoretical studies and with the first experimental description of such nonlinear effects in asymmetric catalytic reactions. Many examples of this nonlinear behavior have since been observed,<sup>6</sup> and the use of non-enantiopure catalyst mixtures is rapidly becoming a common mechanistic tool based on Kagan's work.

Nonlinear behavior in asymmetric catalysis is typically reported as product enantioselectivity ( $ee_{\text{prod}}$ ) vs catalyst enantiomeric excess ( $ee_{\text{cat}}$ ), as shown in Figure 1, where a positive deviation from the linear relationship is termed an "asymmetric amplification" of  $ee_{\text{prod}}$ . Less emphasis has been placed on the consequences for *reaction rate*, although even the earliest discussions of such nonlinear

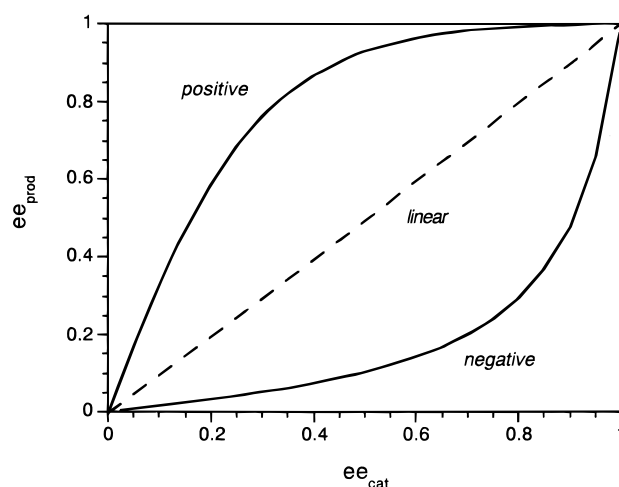
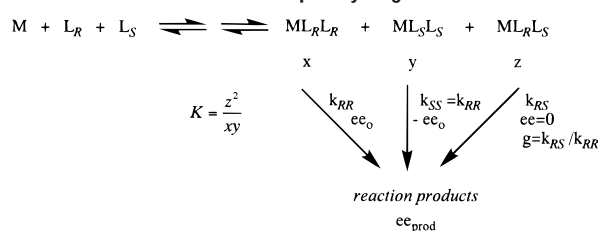


FIGURE 1. Relationships between enantioselectivity of the reaction product ( $ee_{\text{prod}}$ ) and enantiomeric excess of the chiral catalyst ( $ee_{\text{cat}}$ ).

## Scheme 1. $ML_2$ Model Developed by Kagan and Co-Workers<sup>5</sup>



effects noted influences on both product ratio *and* reaction rate.<sup>4</sup> Our work in this area<sup>7</sup> has served to highlight some of the less-well-recognized kinetic aspects of nonlinear behavior in asymmetric catalysis, and this paper summarizes how a kinetic approach complements the models developed by Kagan. In some cases striking consequences are revealed for both chiral and overall synthetic efficiency of reactions carried out using non-enantiopure catalysts or chiral auxiliaries. We demonstrate how consideration of the kinetic behavior may serve to enhance the use of nonlinear effects as a diagnostic tool for identifying active catalytic species and for providing mechanistic insight. Kinetic information may also help in the development of efficient synthetic strategies using non-enantiopure systems.

## Theoretical Models of Nonlinear Effects

Scheme 1 shows the reaction network for the  $ML_2$  model developed by Kagan and co-workers.<sup>5</sup> This simplest of the  $ML_n$  models describes an asymmetric catalytic reaction based on two enantiomeric chiral ligands,  $L_R$  and  $L_S$ , and a metal center,  $M$ . Three different catalyst species, two homochiral complexes and a *meso* complex, may be formed with relative concentrations which are fixed by an equilibrium constant  $K$  (eq 1).  $\beta$  (eq 2) is a parameter which allows  $K$  to be related to the optical purity of the chiral catalyst  $ee_{\text{cat}}$  by eliminating the individual mole

Donna G. Blackmond obtained a Ph.D. in chemical engineering from Carnegie Mellon University in Pittsburgh, PA, in 1984. She was a professor in chemical engineering at the University of Pittsburgh from 1984 to 1992, receiving the NSF Presidential Young Investigator Award (1985–90). From 1992 to 1995 she was an Associate Director at Merck & Co., Inc., Rahway, NJ. She served as a Research Group Leader at the Max-Planck-Institut für Kohlenforschung, Mülheim-Ruhr, Germany, from 1996 to 1999 and received the Max-Planck-Society's Award for Outstanding Women Scientists in 1998. In 1999 she joined the University of Hull, UK, as Professor of Physical Chemistry. She received the Fieser Guest Lectureship from Harvard University in 2000. Her research interests are in kinetic aspects of organic catalytic reactions, particularly asymmetric catalysis.

\* Tel.: +44 1482 46 6401. Fax: +44 1482 46 6410. E-mail: D.G.Blackmond@chem.hull.ac.uk.

fractions of the three complexes ( $x$ ,  $y$ , and  $z$ ) from the equation.

$$K = z^2/xy \quad (1)$$

$$\beta = \frac{z}{x+y} = \frac{-K ee_{\text{cat}}^2 + \sqrt{-4K ee_{\text{cat}}^2 + K(4 + K ee_{\text{cat}}^2)}}{4 + K ee_{\text{cat}}^2} \quad (2)$$

The two enantiopure catalysts  $ML_RL_R$  and  $ML_SL_S$  give identical reaction rates ( $r_{RR} = r_{SS}$ ) and reaction products of opposite enantioselectivities ( $ee_o$  and  $-ee_o$ , respectively). Racemic product is formed from the *meso* catalyst  $ML_RL_S$ , which exhibits a reactivity of  $g$  relative to the enantiopure catalysts ( $g = r_{RS}/r_{RR}$ ). With these definitions, Kagan and co-workers<sup>5</sup> showed that the enantioselectivity of the reaction product obtained from this mixture,  $ee_{\text{prod}}$ , will vary with  $ee_{\text{cat}}$  according to eq 3, through which plots such as Figure 1 are obtained.

$$ee_{\text{prod}} = ee_o ee_{\text{cat}} \frac{1 + \beta}{1 + g\beta} \quad (3)$$

The parameters  $K$  and  $g$  provide hints about the nature of the catalyst mixture at varying relative amounts of  $L_R$  and  $L_S$ . A value of  $K = 4$  gives a statistical distribution of ligands between the three complexes; larger values indicate predominance of the *meso* species. The parameter  $K$  is an inherent property of the catalyst mixture, independent of  $ee_{\text{cat}}$ , while  $\beta$  varies with  $ee_{\text{cat}}$ .  $K$  is also independent of the catalytic reaction itself, and therefore independent of the parameter  $g$ . Values of  $g$  less than 1 indicate that the *meso* species is a less active catalyst than is the enantiopure species for that particular reaction. Different reactions carried out with the same catalyst mixture should afford the same value of  $K$  but possibly different values of  $g$ .

In many experimental cases where catalysts are formed in situ by addition of M and L to the reaction mixture, physical identification of the different species which are formed can be problematic if not impossible. The beauty of Kagan's models lies in their use of data describing the reaction event itself to extract information independent of the reaction.

**Role of Reaction Rate.** We recently showed that the models developed by Kagan allow derivation of not only a *ratio* of the three catalyst species  $x$ ,  $y$ , and  $z$  (eqs 1 and 2) but also their absolute relative proportions at any value of  $ee_{\text{cat}}$ .<sup>7a</sup> Thus, the overall reaction rate for the mixed system may be described in terms of the reaction rate for the enantiopure system,  $r_{RR}$ , as shown in eq 4.

$$r = (x + y + gz)r_{RR} \quad (4)$$

The role of reaction rate in systems exhibiting nonlinear effects may be demonstrated by considering cases exhibiting positive and negative nonlinear effects. Figure 2a shows a strong asymmetric amplification in product enantioselectivity, similar to the striking experimental results of Noyori et al.<sup>8</sup> in the DAIB-catalyzed nucleophilic addition of dialkylzinc to aldehydes, which Kagan has

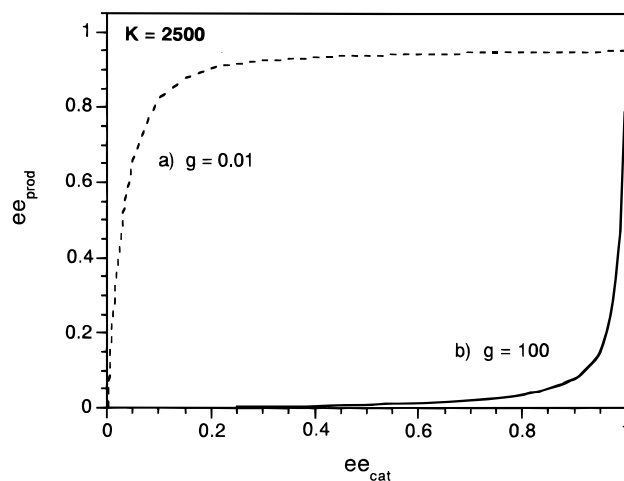


FIGURE 2.  $ee_{\text{prod}}$  vs  $ee_{\text{cat}}$  simulated for the  $ML_2$  model<sup>5</sup> with  $K = 2500$ . The system is modeled for two extreme cases of reactivity of *meso* species: (a)  $g = 0.01$  and (b)  $g = 100$ .

analyzed according to the  $ML_2$  model.<sup>9</sup> This example is appealing since it demonstrates that a product of extremely high enantioselectivity may be derived from a nearly racemic catalyst mixture. What if this same catalyst instead exhibited the negative nonlinear effect shown in Figure 2b? Most synthetic chemists would aim to avoid this case where a nearly racemic product is derived from catalyst mixtures of high enantiomeric excess.

The reaction rates predicted in Figure 3 present a strikingly different view of the overall synthetic efficiency compared to consideration of enantioselectivity alone. For example, at 10%  $ee_{\text{cat}}$ , if the enantiopure catalyst produces a certain amount of the *desired* enantiomer in 1 day, the case of asymmetric amplification in Figure 2a will require 10 days to produce the same amount. By contrast, the system exhibiting a strong negative nonlinear effect (Figure 2b) takes only half an hour to produce the same amount of *desired* enantiomer that requires 1 day to produce when the catalyst is used in enantiopure form.

Thus, in the  $ML_2$  model a strong positive nonlinear effect in product enantioselectivity comes at the cost of a severely suppressed reaction rate compared to the enantiopure case. Conversely, a negative nonlinear effect yields higher productivity of the *desired* enantiomer than may be achieved using the enantiopure catalyst.

The nonlinear effect is the result of an in situ purification of the active enantiopure catalyst through diversion of a large fraction of the minor ligand to the *meso* species; however, since the same absolute amount of the major ligand is also sacrificed in this process, the amount of catalyst ultimately available for carrying out the enantioselective reaction can be significantly decreased. If the *meso* species is significantly less active than the enantiopure catalyst, an asymmetric amplification in product enantioselectivity is observed with a concomitant decrease in reaction rate.

Figure 3 shows that the difference in reactivity for a mixed  $ee$  system compared to the enantiopure system lessens as  $ee_{\text{cat}}$  increases. Therefore, synthetically useful examples of asymmetric amplification may be envisioned for reactions employing non-enantiopure mixtures at

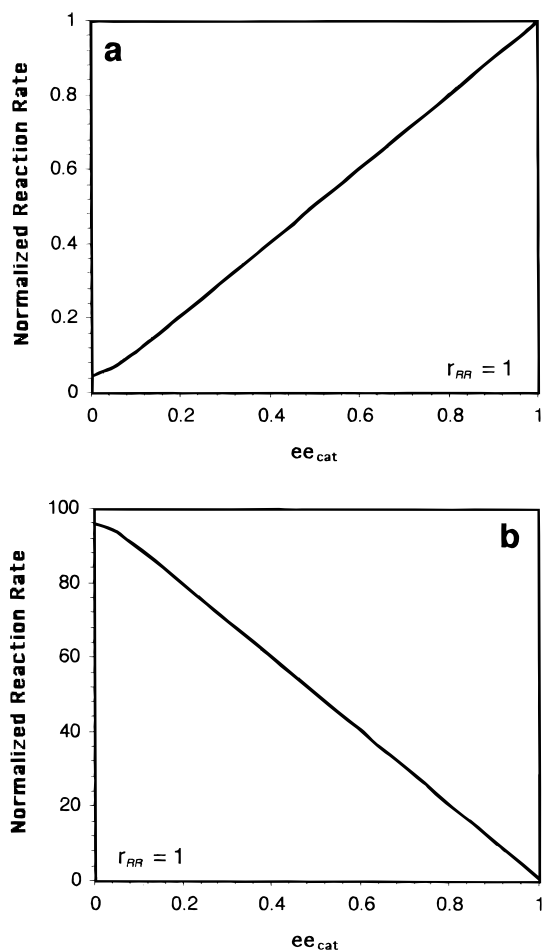
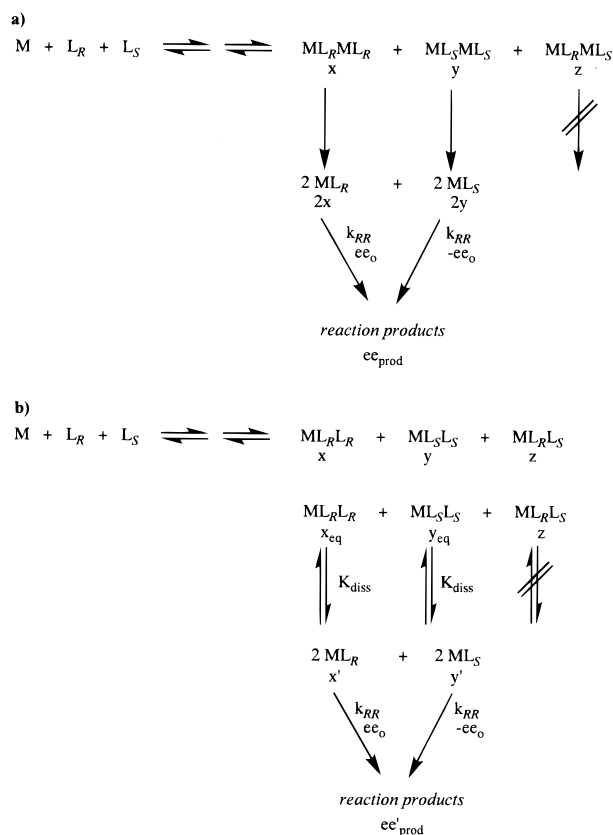


FIGURE 3. Reaction rate predicted from the  $ML_2$  model<sup>5</sup> for the cases shown in Figure 2. The rate as a function of  $ee_{cat}$  is compared to the enantiopure catalyst with  $r_{RR} = 1$ . (a)  $g = 0.01$  and (b)  $g = 100$  (see refs 7a,c).

higher values of  $ee_{cat}$  which do not carry such a significant penalty in overall productivity.<sup>10</sup> Combining information concerning enantioselectivity and reaction rate allows a more informed choice of synthetic route. In cases where productivity is paramount, and a viable separation process exists, a system exhibiting a strong negative nonlinear effect may indeed prove more efficient than a case of asymmetric amplification.<sup>11</sup>

**Reaction Rate as a Mechanistic Tool.** The goodness of the fit of the enantioselectivity data to models such as those developed by Kagan implies the degree of confidence one has in the proposed mechanistic picture of the catalytic system. Often independent evidence concerning the nature of the catalytic complexes is sought, such as molecular weight measurements or X-ray structural analysis. In a similar way, comparison of experimental and predicted values for reaction rate can provide further corroboration. Reaction rate as a diagnostic tool offers an advantage over methods such as those cited above in that it provides direct information about the active catalyst species under the relevant reaction conditions. Unfortunately, kinetic information about reactions exhibiting nonlinear effects is scarce and, when available, is usually qualitative and given only for a limited number of  $ee_{cat}$  values.

#### Scheme 2. $ML_2$ Models Modified for Monomeric Active Species: (a) Irreversible Dissociation and (b) Reversible Dissociation



Many literature reports have appeared for systems showing positive nonlinear effects which are attributed to the formation of dimeric species in agreement with the  $ML_2$  model. Generally, qualitative agreement with the rate suppression described above has been found. If, however, the predicted and experimental rates are not in quantitative agreement, the assumptions of the model may be examined. The models are based on the formation in solution of reactive dimeric species whose relative concentrations are given by an equilibrium distribution which is fixed prior to the reaction and is not affected by the reaction. It is also assumed that all catalytic species in the mixture exhibit the same kinetic rate law, and that enantioselectivity is not conversion-dependent. The next sections of this paper discuss how kinetic information may help to provide mechanistic insight in examples where one of these assumptions has clearly broken down.

### Monomeric vs Dimeric Active Species

**Theoretical Models.**<sup>12</sup> It has been suggested in a number of reports of nonlinear effects that the active catalytic species is, in fact, monomeric in the chiral ligand. Kagan proposed that a modified version of the  $ML_2$  model could still be used to rationalize the nonlinear behavior in cases where active monomeric species are formed from dissociation of dimeric species under reaction conditions.<sup>5b</sup> We develop here two variations of this model (Scheme 2a and b). We assume that three dimeric species are first established in solution in the absence of the reactants at

a fixed relative concentration set by  $K$  as described by the  $ML_2$  model. Both models shown in Scheme 2 require that the dimers no longer undergo exchange with each other under reaction conditions, an assumption which has been verified in some cases.<sup>13</sup> In accordance with a number of experimental reports, we assume that the *meso* species is much more stable than the homochiral species. Under the conditions of the catalytic reaction, therefore, the *homo-chiral* species *only* dissociate irreversibly (Scheme 2a) or reversibly (Scheme 2b) to form the monomeric species, which then take part in the catalysis. For irreversible and complete dissociation, the equations of the original  $ML_2$  model (eqs 3 and 4) with  $g = 0$  may be used to describe the nonlinear effect in  $ee_{\text{prod}}$  and rate. When dissociation of the homochiral dimers is reversible and in equilibrium (Scheme 2b), eq 5 shows how the relative amounts of active monomeric catalysts  $x'$  and  $y'$  will be related to the original concentrations of dimers ( $x$  and  $y$ ) fixed by the  $ML_2$  model.

reversible dissociation

$$x = x' + x_{\text{eq}} = x' + (x')^2/K_{\text{diss}} \quad (5)$$

$$y = y' + y_{\text{eq}} = y' + (y')^2/K_{\text{diss}}$$

Enantioselectivity and reaction rate may be predicted by eqs 6a and 6b for this reversible case.

reversible dissociation  $ee'_{\text{prod}} = ee_{\text{o}} \frac{x' - y'}{x' + y'}$  (6a)

reversible dissociation  $r = [x' + y']r_{\text{RR}}$  (6b)

The two models shown in Scheme 2 predict different relative amounts of the active monomeric  $R$  and  $S$  species at any given value of  $ee_{\text{cat}}$ , and thus predict different nonlinear relationships between  $ee_{\text{cat}}$  and  $ee_{\text{prod}}$  and between  $ee_{\text{cat}}$  and rate, as illustrated in Figures 4 and 5. In general, reversible dissociation ameliorates the potential for asymmetric amplification which is fixed in the original dimer formation process. Indeed, the reversible model can predict a nearly *linear* relationship in enantioselectivity and rate as a function of  $ee_{\text{cat}}$ , even for the same original distribution of homochiral and heterochiral species which would give a nonlinear effect when dissociation is irreversible (Figures 4a and 5a,  $K = 4$ ,  $K_{\text{diss}} = 0.01$ , compared to the solid line). The reversible dissociation model approaches the irreversible model at large  $K_{\text{diss}}$  values, where the system is driven strongly toward monomeric species. At a given  $K$  value, the fraction of the total ligand concentration actually participating in the reaction is smaller for reversible dissociation than for irreversible dissociation. It may also be noted that, for a given  $K$  value, the reversible model predicts a smaller suppression of reaction rate with decreasing  $ee_{\text{cat}}$ .

Thus, the subtleties of the interplay between species in solution may have a significant influence on the observed catalytic behavior. In the absence of corroborating information about the nature of the species present and their interactions in solution, it may not be clear which model best describes a given reaction. Consider a

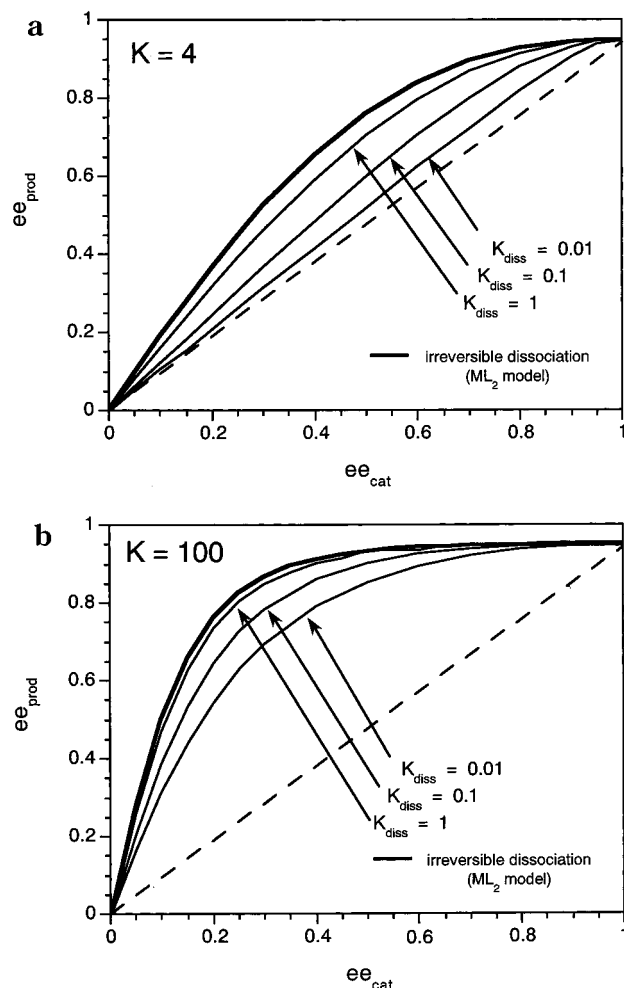


FIGURE 4.  $ee_{\text{prod}}$  vs  $ee_{\text{cat}}$  predicted from the irreversible (Scheme 2a) and reversible (Scheme 2b) models for monomeric active species. (a)  $K = 100$  and (b)  $K = 4$ .

mixture of dimeric species formed according to the original  $ML_2$  model with  $K = 20$ . Let us assume that under reaction conditions the solution consists of a stable *meso* species (at a concentration set by  $K$ ) and homochiral dimers in equilibrium with catalytically active monomeric  $R$  and  $S$  species (as in Scheme 2b) with dissociation equilibrium constant  $K_{\text{diss}} = 0.1$ . The filled circles in Figure 6a represent simulation of data for this system for different values of  $ee_{\text{cat}}$ . The solid line in Figure 6a represents *not* the fit to this model but instead a fit of these data points to the standard  $ML_2$  model with  $K = 4$  and  $g = 0$  (as in Scheme 2a). Although the agreement is good, the data points and the curve fit describe very different chemistry. However, kinetic measurements might help distinguish between the two models, because as shown in Figure 6b, the two models exhibit different reaction rate behavior as a function of  $ee_{\text{cat}}$ . Accurate measurements of reaction rate as a function of  $ee_{\text{cat}}$  might therefore be used to help choose between different mechanistic proposals.

One interesting implication of the reversible model described in Scheme 2b is that the chemistry of the reaction itself can affect the amounts of the species present within the catalytic cycle, unlike in the original  $ML_n$  models for dimeric active species. Since the *meso*



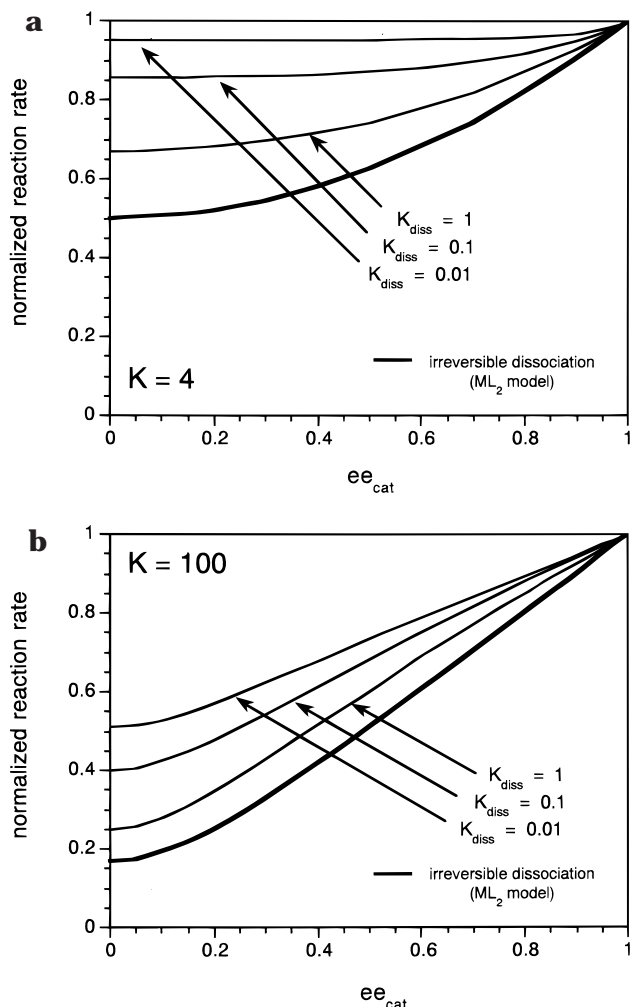
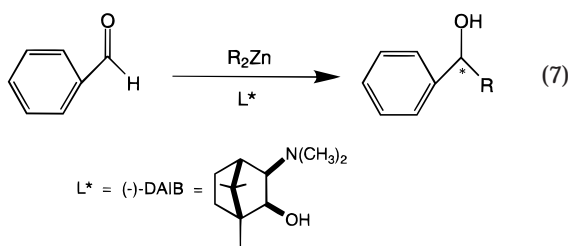


FIGURE 5. Reaction rate vs  $ee_{cat}$  predicted from the irreversible (Scheme 2a) and reversible (Scheme 2b) models for monomeric active species. (a)  $K = 100$  and (b)  $K = 4$ .

complex is removed from the system in this model, these kinetic considerations will not affect the observed nonlinear behavior. The general case where the *meso* species remains involved in the dynamic monomer–dimer equilibria is treated by Noyori and co-workers in their more complex model for monomeric active species (see next section).<sup>8</sup>

#### Nucleophilic Addition of Dialkylzinc to Aldehydes.

One of the most notable early examples of nonlinear effects was the nucleophilic addition of dialkylzinc to aldehydes mediated by chiral  $\beta$ -amino alcohols such as DAIB, first observed by Oguni and co-workers<sup>14</sup> (eq 7). This



system has been studied extensively by Noyori and co-workers<sup>8</sup> using kinetic, spectroscopic, and structural mea-

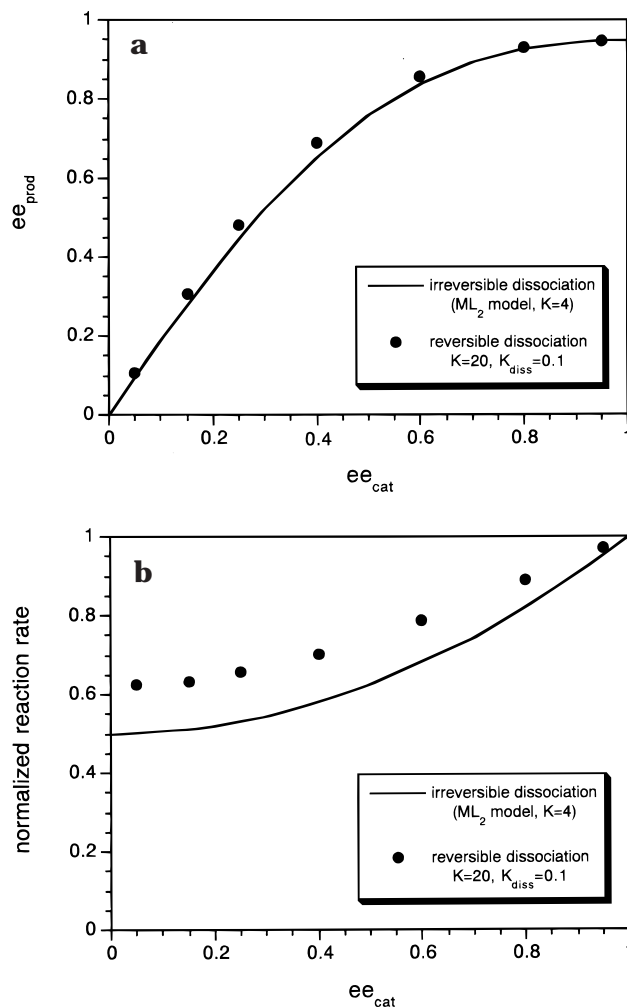
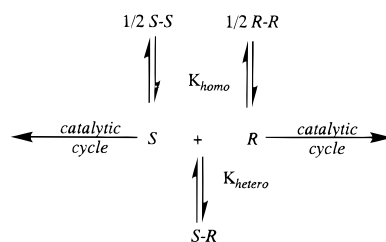


FIGURE 6. Comparison of predicted (a)  $ee_{prod}$  and (b) reaction rates vs  $ee_{cat}$  for the irreversible model (Scheme 2a) with  $K = 4$  and the reversible model (Scheme 2b) with  $K = 20$ .

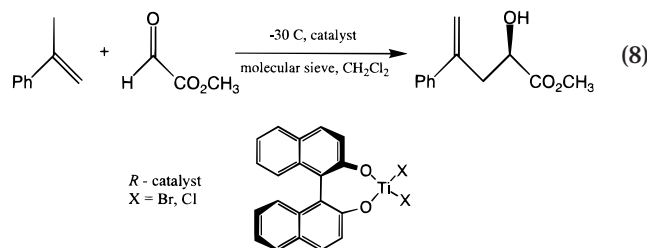
#### Scheme 3. Relationship between Catalytically Active Monomeric and Inactive Dimeric Species (Eq 7, Ref 13b)



surements as well as kinetic modeling and reaction simulations. They presented a separate mathematical analysis with important distinctions from the  $ML_2$  models.<sup>8b</sup> They proposed that the system involves a complex balance between monomeric and dimeric species which remain in equilibrium over the course of the reaction, with entry into the catalytic cycle through the monomeric ML. Homochiral dimeric species are required to pass through monomeric species in order to form the *meso* species as shown in Scheme 3. This model also dictates that the concentration of monomeric ML species engaged in catalysis at any point during the reaction will depend on the concentrations of reactants at that point. Therefore,

the relative amounts of the various dimeric (ML)<sub>2</sub> species will change during the reaction in a complex way related to the kinetic rate law for the reaction. In systems where *R* and *S* ligands are present in unequal amounts, the product enantioselectivity should thus depend on the concentration of the substrate. Although this prediction did not match experimental observations,<sup>8b</sup> the discrepancy was rationalized in terms of product inhibition which could prevent release of the monomeric species to undergo further catalytic cycles. In this case a corresponding decrease in reaction rate should be expected, but this has not been tested experimentally. Thus, it is clear that despite the extensive study of this complex system, further kinetic studies could help to address remaining mechanistic questions.<sup>15</sup>

**Glyoxylate-Ene Reaction.** Mikami and co-workers<sup>16</sup> have studied the glyoxylate-ene reaction mediated by chiral Lewis acids synthesized from Ti(OiPr)<sub>2</sub>Cl<sub>2</sub> and 1,1'-binaphthol (BINOL) of varying enantiomeric excess (eq 8). Molecular weight measurements suggested that dimer-



ic species are formed. A concentration dependence of molecular weight was found for the homochiral species but not the racemic mixture, further suggesting that the heterochiral dimer species was the significantly more stable species. A strong positive nonlinear effect was observed in the reaction, and the enantiopure catalyst was 35 times more active than the racemic mixture. The authors proposed a reaction mechanism which requires dissociation of the dimeric species in binding to the glyoxylate.<sup>16a</sup> They also proposed that a trinuclear species may form, and their recent work confirms this and suggests that it may be the active catalyst precursor.<sup>16b</sup>

A good fit may be obtained by application of either of the modified ML<sub>2</sub> models of Scheme 2a and b with different parameters as shown in Figure 7. The large value of the ML<sub>2</sub> model parameter *K* in either case supports the authors' suggestion from molecular weight measurements that the *meso* dimer is more stable than the homochiral species, and the experimental trend in rate behavior is in qualitative agreement. However, both models of Scheme 2 predict a smaller suppression of activity for the reaction using a racemic mixture than that noted experimentally.<sup>17</sup> This difference might be rationalized if the reversible dissociation did not reach equilibrium, giving a steady-state concentration of monomeric species smaller than predicted. Further, the modified ML<sub>2</sub> models could account for any inactive higher order species formed,<sup>16b</sup> and a correspondingly lower rate would be observed.

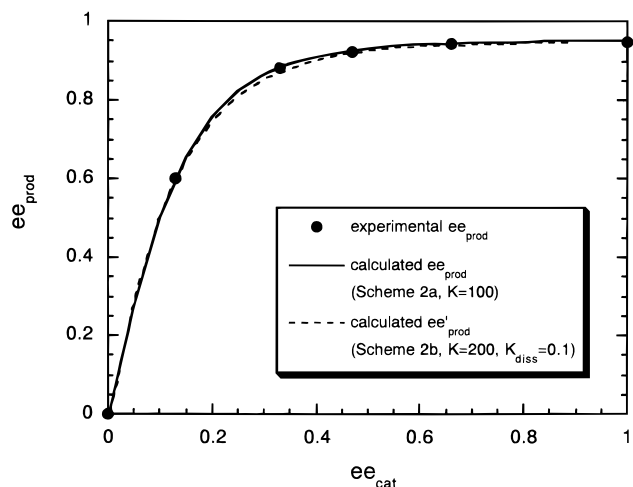
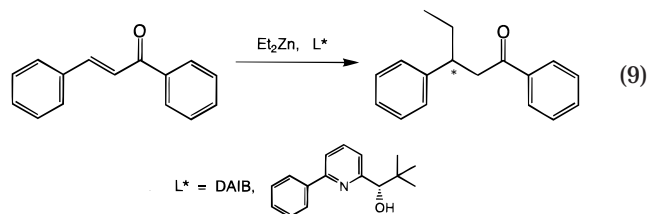


FIGURE 7. Modified ML<sub>2</sub> models of Scheme 2a and b applied to data from the glyoxylate-ene reaction (eq 8, ref 16).

## Conversion Dependence of Enantioselectivity

**Conjugate Addition of Dialkylzinc to Chalcones.** Nonlinear effects have been observed in the alkylation of unsaturated enones using dialkylzinc to form  $\beta$ -substituted carbonyl compounds (eq 9). Catalytic versions of



these reactions are mediated by Ni complexes prepared using chiral amino alcohols such as DAIB<sup>18</sup> or substituted pyridine and bipyridine derivatives.<sup>19</sup> Both Bolm and co-workers<sup>19</sup> and Feringa and co-workers<sup>18</sup> observed strong positive nonlinear effects in this reaction. However, both groups also noted that product enantioselectivity was sensitive to other variables, including conversion,<sup>18,19</sup> Ni content,<sup>18</sup> and ligand concentration.<sup>19</sup> It was speculated that these effects may be due to the slow dissociation of an inactive *meso* complex or the production of other nonselective catalytic Ni species over time.

A dependence of enantioselectivity on conversion suggests that the point during reaction at which an observation is made is a crucial consideration. However, the effects of reaction variables on enantioselectivity were not monitored at constant conversion. When we plot the data from both studies together in terms of product yield, as in Figure 8, it may be seen that in each case a sharp drop in product enantioselectivity is consistently observed at high (ca. 80%) yield. This idea also fits well with the change in enantioselectivity observed as a function of reaction progress in both studies. We plot their data as "incremental" enantioselectivity<sup>20</sup> vs conversion in Figure 9, revealing that the decrease in catalyst enantioselectivity, particularly at the end of the reaction, is more significant than is apparent from the cumulative values. In fact, during the last 5% conversion in the reaction shown in

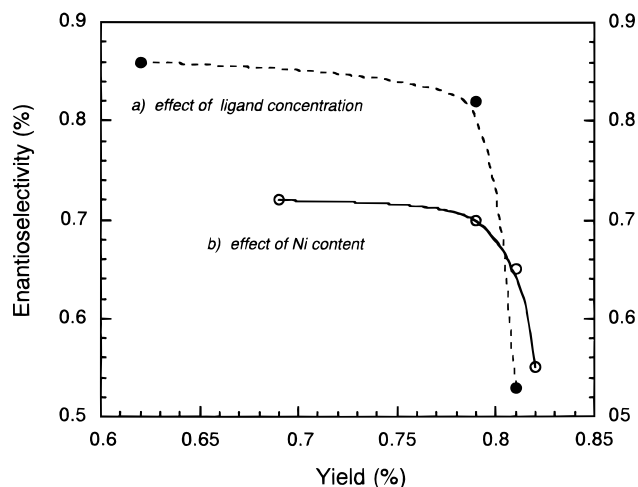


FIGURE 8.  $ee_{\text{prod}}$  vs yield in the addition of dialkylzinc to chalcone (eq 9). Data were extracted from refs 18 and 19.

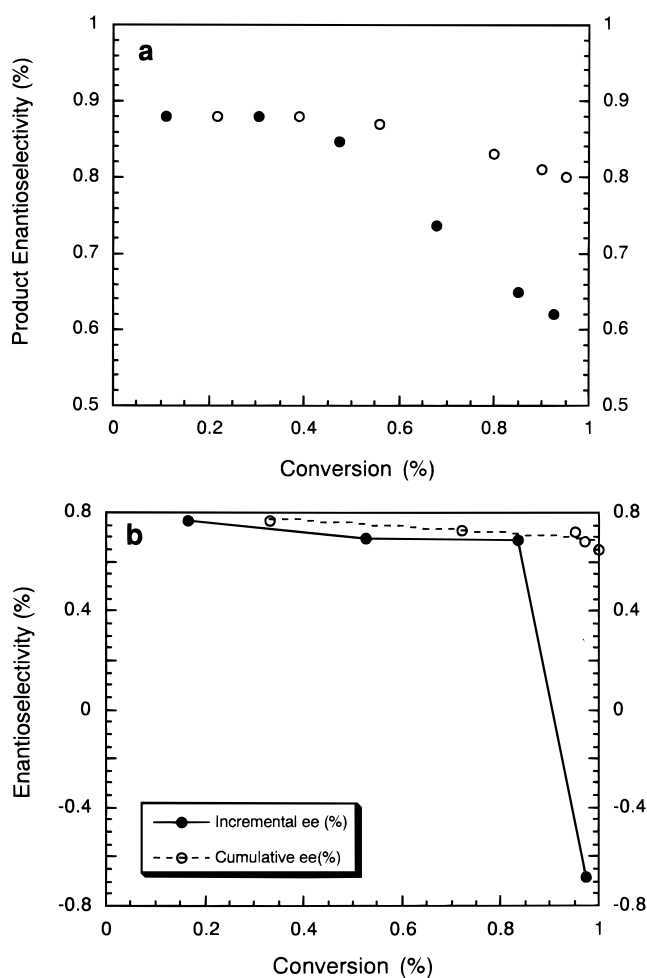


FIGURE 9.  $ee_{\text{prod}}$  vs conversion in the addition of dialkylzinc to chalcone (eq 9). Incremental  $ee_{\text{prod}}$  was calculated in this work. Cumulative  $ee_{\text{prod}}$  was taken from (a) ref 19 and (b) ref 18.

Figure 9b, we find that the enantioselectivity completely inverted from 68% ee *R*-product to 68% ee *S*-product!

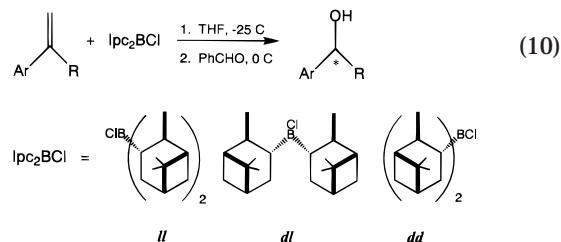
These trends are not easily explained by the simple assumption that deactivation or agglomeration of the chiral species to form nonselective Ni catalysts occurs over time, but they suggest instead that the presence of

substrate plays a role in the enantiodifferentiation in this reaction.<sup>21</sup> Feringa noted that in the absence of Ni, the catalytic reaction occurred slowly to give the opposite product, presumably with organozinc complexes of the chiral ligand effecting the reaction. The results shown in Figures 8 and 9 might be explained by the models of Scheme 2, where the homochiral and heterochiral Ni dimer species form active monomers only in the presence of substrate. If the Ni species is shifted toward stable and inactive dimers (both homochiral and heterochiral) at low substrate concentrations, organozinc species may begin to compete as catalysts, giving enantioselectivities very different from those of the monomeric Ni complex which dominated at higher substrate concentrations.

Detailed kinetic measurements will be needed to test hypotheses such as these. It is clear from these data, however, that close attention to and control of kinetic variables such as conversion are required for systematic investigation of the influence of reaction variables, and for the development of rational mechanistic interpretations derived from investigations of nonlinear effects.

**Nonlinear Effects in Stoichiometric Asymmetric Reactions.** In reactions using stoichiometric reagents which exhibit nonlinear effects, a number of special considerations arise because the chiral auxiliary is consumed in the reaction. In a system following the  $ML_2$  model, if the *meso* species possesses nonzero activity and if this activity is different from that of the homochiral species (if  $g \neq 0$  and  $g \neq 1$ ), the homochiral and heterochiral species will be consumed at different rates, and the reaction will exhibit a conversion-dependent enantioselectivity. If a stoichiometric amount of the chiral reagent is used, the nonlinear effect (either positive or negative) will be eroded as conversion increases, and the product enantioselectivity at 100% conversion will necessarily be a linear reflection of the enantiomeric excess of the chiral auxiliary.

These concepts are illustrated below in the example of the stoichiometric reduction of aralkyl ketones (eq 10) using non-enantiopure  $Ipc_2BCl$ , a chiral borane compound originally introduced by H. C. Brown.<sup>22</sup> Scientists



at Merck<sup>23</sup> found that the use of  $Ipc_2BCl$  prepared from 85% ee  $\alpha$ -pinene was as effective in producing highly enantiopure alcohols as was the more expensive 97% ee starting material. This asymmetric amplification was accompanied by a conversion-dependent enantioselectivity, as shown by the filled and open symbols in Figure 10. While an  $ML_2$  fit to enantioselectivity data at high conversion would not be meaningful, a fit to their data collected at the beginning of the reaction (solid line in Figure 10) allows us to determine the relative *initial*

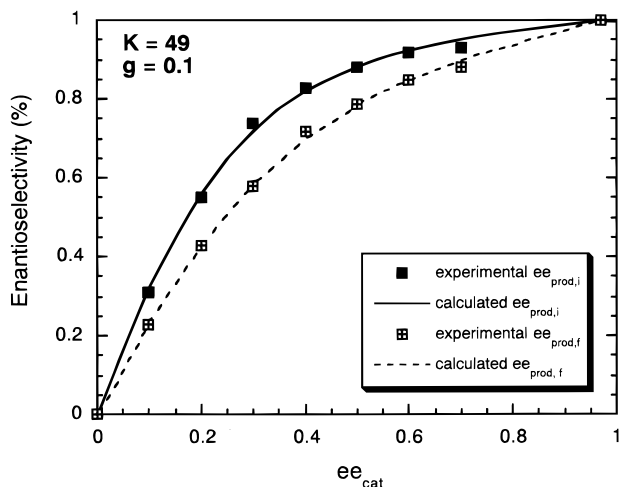


**FIGURE 10.** Experimental and calculated  $ee_{\text{prod}}$  in the  $\text{Ipc}_2\text{BCl}$ -mediated stoichiometric reduction of aralkyl ketones (eq 10). Experimental data are from ref 23. Calculation of  $ee_{\text{prod},f}$  was done from separate reaction simulations at each  $ee_{\text{cat}}$  using the parameters obtained in the fit to the initial  $ee$  data (see ref 7b).

concentrations of the different chiral species and enables us to trace their fates over the course of the reaction.<sup>7b</sup> The model suggested that the *meso* species is formed in higher than the statistical distribution assumed in ref 23 and that it exhibits about 10% of the activity of the homochiral species. Simulation of the reaction on the basis of these initial parameters then allows us to predict the enantioselectivities at higher conversion for reactions using mixtures of different enantiopurities of  $\text{Ipc}_2\text{BCl}$ , shown as the dotted line in Figure 10.<sup>7b</sup> This result is *not* a fit to the final  $ee$  data but is *predicted* from the initial  $ee$  data. Therefore, the excellent agreement between the experimental and predicted data provides an independent corroboration of the proposed  $\text{ML}_2$  mechanistic hypothesis in this reaction.

Figure 11 illustrates the influence of conversion on  $ee_{\text{prod}}$  and the relative concentrations of the homochiral and heterochiral species for the simulation of the reaction using  $ee_{\text{aux}} = 0.3$ . Asymmetric amplification is observed at lower conversions where the concentration of the more active and selective homochiral species is higher (Figure 11a); however, as this species is consumed, conversion to the product will ultimately be completed by the less active *meso* fraction unless the chiral reagent is present in excess. In effect, the reaction is a kinetic resolution of the *meso* species. At high conversions the reaction produces racemic product, and the cumulative enantioselectivity ultimately reaches that of the chiral auxiliary (Figure 11b). This inexorable erosion of the asymmetric amplification may be combated by judicious selection of excess chiral reagent determined from an  $\text{ML}_2$  model fit of *initial* enantioselectivity data. In a case where the *meso* species is completely inactive, while no erosion of enantioselectivity will be observed, a properly chosen excess amount of chiral reagent will nevertheless be required in order to achieve full conversion of the substrate.<sup>7b</sup>

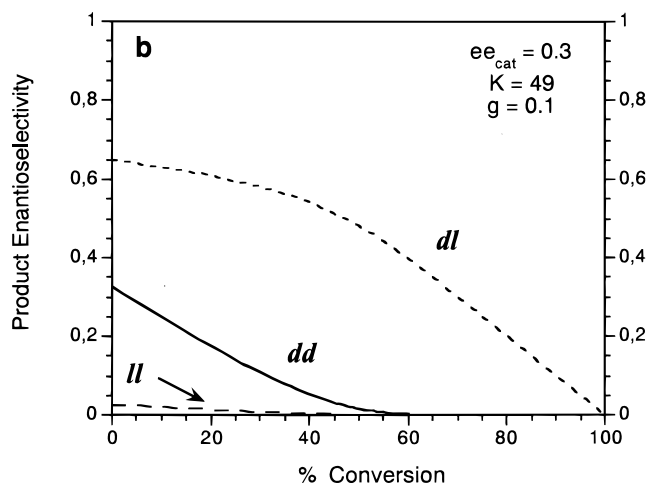
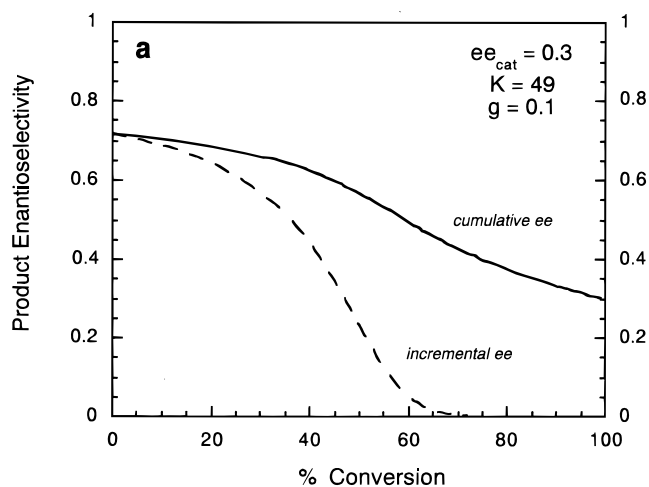
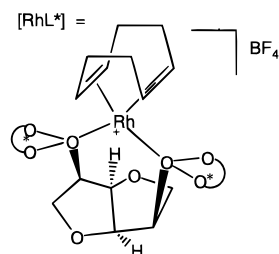
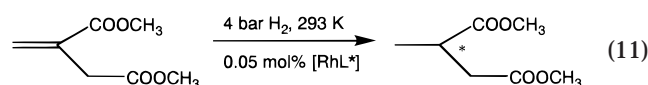


**FIGURE 11.** Influence of conversion on (a)  $ee_{\text{prod}}$  and (b) relative concentrations of *dd*, *ll*, and *dl* species in the stoichiometric reduction of aralkyl ketones (eq 10) for  $ee_{\text{cat}} = 0.3$  (see ref 7b).

## Nonlinear Effects in Diastereomeric Catalyst Mixtures

A related type of nonlinear effect concerns reactions using mixtures of diastereomeric catalysts which lead to reaction products of opposite absolute configuration.<sup>24</sup> We recently studied mixtures of the diastereomeric catalysts shown in eq 11 in the asymmetric hydrogenation of the dimethyl



product enantioselectivities:

<i>R,R</i> catalyst 1:	92.4 %ee ( <i>R</i> )
<i>S,S</i> catalyst 2:	89.4 %ee ( <i>S</i> )
50% <i>R,R</i> catalyst 1:	
+ 50% <i>S,S</i> catalyst 2:	54.8 %ee ( <i>S</i> )

(\*) = chiral ligand  $\text{L}^*$

$\text{L}^* = (\text{R,R})$  binaphthyl: *R,R* catalyst 1  
 $= (\text{S,S})$  binaphthyl: *S,S* catalyst 2



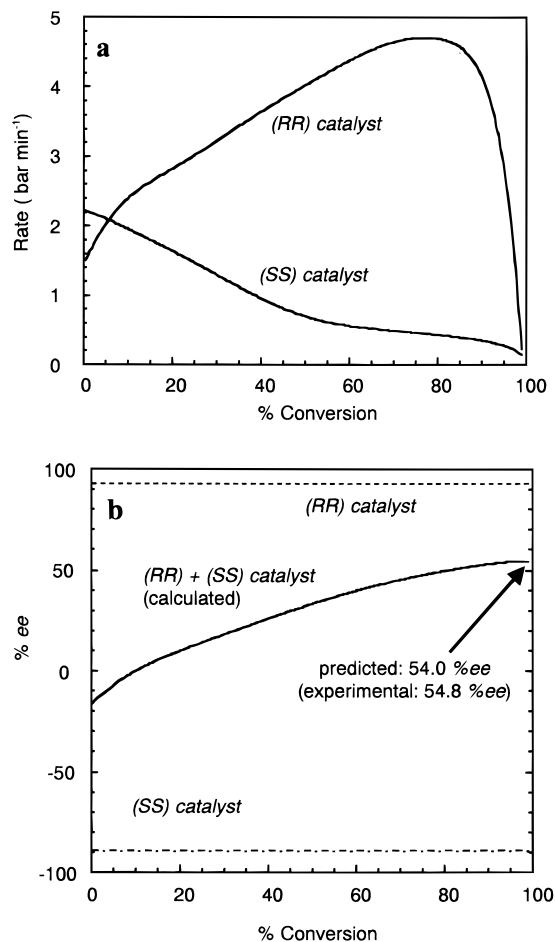


**FIGURE 12.** Asymmetric hydrogenation of itaconic acid as shown in eq 11. (a) Experimental rate vs conversion for reactions using pure ligands. (b) Calculated  $ee_{\text{prod}}$  vs conversion for reaction using 50% *RR* catalyst, 50% *SS* catalyst, compared to experimental endpoint value (see ref 7d).

ester of itaconic acid.<sup>7d,25</sup> In separate reactions, the two catalysts gave high and opposite product enantioselectivities and quantitative yield (*RR*-catalyst, 92.4% ee *R*-product, and *SS*-catalyst, 89.4% ee *S*-product). It was confirmed that the enantioselectivity obtained using either pure catalyst alone did not vary with conversion of substrate. A 1:1 mixture of the two catalysts also gave quantitative yield, but, interestingly, the final product enantioselectivity was 54.8% ee *R*-product. The reaction rate curves shown in Figure 12a for reactions using the catalysts separately reveal that they exhibit strikingly different kinetic profiles. Figure 12b shows that the calculated enantioselectivity, under the assumption that the catalysts act independently in the mixture, predicts a shift from 16% ee *S*-product to 54% ee *R*-product, in excellent agreement with the experimentally determined endpoint value.<sup>7d</sup> Thus, the observed nonlinear effect was not diagnostic of interaction between the catalysts to form new dimeric or higher order species.

A similar example was recently reported by Bolm and co-workers<sup>26</sup> in the nucleophilic addition of dialkylzinc to benzaldehyde (see eq 8) catalyzed by the planar-chiral ferrocenyl ligands shown in Figure 13. When nonequal mixtures of the two diastereomeric catalysts were em-

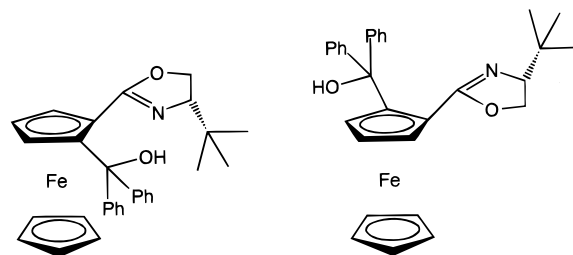


**FIGURE 13.** Diastereomeric ligands from ref 26 used in the nucleophilic addition of dialkylzinc to benzaldehyde (eq 7).

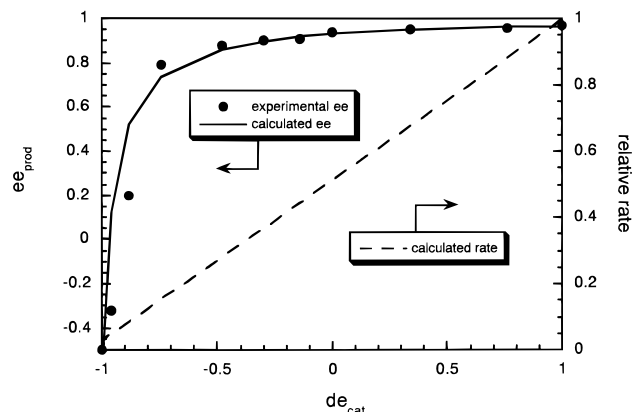


**FIGURE 14.** Experimental (ref 26)  $ee_{\text{prod}}$  and calculated (this work)  $ee_{\text{prod}}$  and reaction rate as a function of  $de$  in the nucleophilic addition of dialkylzinc to benzaldehyde (see Figure 13, eq 7).

ployed, the product enantioselectivity was not a linear reflection of the diastereomeric excess of the catalyst mixture, as shown in Figure 14. Calculation of product enantioselectivity, assuming that the catalysts exhibit the same rate law, shows that the nonlinear effect may be attributed to the significantly different activities exhibited independently by the two catalysts following the same rate law. Enantioselectivity is expected to be independent of conversion. Bolm<sup>26</sup> suggested that a practical application of the asymmetric amplification shown in Figure 14 may be in avoiding additional separation steps in ligand preparation. It should be noted, however, that calculated rate of Figure 14 predicts that a 50:50 mixture of diastereomers will require twice as long to complete the reaction compared to the diastereomerically pure catalyst.

## Concluding Remarks

The examples in this paper illustrate that profound kinetic consequences may ensue when non-enantiopure catalysts are employed in asymmetric synthesis. In many cases, a strong amplification in product enantioselectivity comes at a significant cost to the overall productivity of the reaction. Further, it is shown how reaction rate measurements may be used to help distinguish between proposed mechanistic hypotheses and proposed catalytically active species, as well as to add insight in cases where complex behavior, including conversion-dependent enantioselectivity, is observed. These kinetic concepts should also be considered in related examples outside the scope of this review, including asymmetric autocatalysis and chiral activation, in which high enantioselectivity is achieved

through an amplification of reaction rate in addition to a diversion of product selectivity. A kinetic approach broadens our fundamental understanding of these reactions and aids in developing efficient synthetic strategies for reactions using non-enantiopure catalysts.

Support from the Max-Planck Institut für Kohlenforschung and the Max-Planck Gesellschaft (Sonderprogramm zur Förderung hervorragender Wissenschaftlerinnen) and Pfizer Central Research is gratefully acknowledged. The author thanks M.T. Reetz, T. Rosner, T. Neugebauer, A.B.E. Minidis, (all MPI), J.R. Sowa, Jr. (Seton Hall University), and M. Terada (Tokyo) for stimulating discussions and collaborations.

## References

- Horeau, A.; Guetté, J. P. Interactions Diastereomeres D'Antipodes en Phase Liquide. *Tetrahedron* **1974**, *30*, 1923–1931.
- Horeau, A. Interactions D'Enantiomeres en Solution: Influence sur le Pouvoir Rotoire: Pureté Optique et Pureté Enantiomérique. *Tetrahedron Lett.* **1969**, *36*, 3121–3124.
- Williams, T.; Pitcher, R. G.; Bommer, P.; Gutzwiller, J.; Uskovic, M. Diastereomeric Solute–Solute Interactions of Enantiomers in Achiral Solvents. Nonequivalence of the Nuclear Magnetic Resonance Spectra of Racemic and Optically Active Dihydroquinine. *J. Am. Chem. Soc.* **1969**, *91*, 1871–1872.
- Wynberg, H.; Feringa, B. Enantiomeric Recognition and Interactions. *Tetrahedron* **1976**, *32*, 2831–2834.
- (a) Puchot, C.; Samuel, O.; Duñach, E.; Zhao, S.; Agami, C.; Kagan, H. B. Nonlinear Effects in Asymmetric Synthesis. Examples in Asymmetric Oxidations and Aldolization Reactions. *J. Am. Chem. Soc.* **1986**, *108*, 2353–2357. (b) Guillaneux, D.; Zhao, S. H.; Samuel, O.; Rainford, D.; Kagan, H. B. Nonlinear Effects in Asymmetric Catalysis. *J. Am. Chem. Soc.* **1994**, *116*, 9430–9439.
- Recent reviews: (a) Girard, C.; Kagan, H. B. Nonlinear Effects in Asymmetric Synthesis and Stereoselective Reactions: Ten Years of Investigation. *Angew. Chem.* **1998**, *110*, 3088–3127; *Angew. Chem., Int. Ed.* **1998**, *37*, 2922. (b) Kagan, H. B.; Girard, C.; Guillaneux, D.; Rainford, D.; Samuel, O.; Zhang, S. Y.; Zhao, S. H. Nonlinear Effects in Asymmetric Catalysis: Some Recent Aspects. *Acta Chem. Scand.* **1996**, *30*, 345–352. (c) Avalos, M.; Babiano, R.; Cintas, P.; Jiménez, J. L.; Palacios, J. C. Nonlinear Stereochemical Effects in Asymmetric Reactions. *Tetrahedron Asymmetry* **1997**, *8*, 2997–3017. (d) Bolm, C. Nonlinear Effects in Enantioselective Synthesis: Asymmetric Amplification. In *Advanced Asymmetric Synthesis*; Stephenson, G. R., Ed.; Blackie A&P: Glasgow, 1996; pp 9–26.
- (a) Blackmond, D. G. Mathematical Models of Nonlinear Effects in Asymmetric Catalysis: New Insights Based on the Role of Reaction Rate. *J. Am. Chem. Soc.* **1997**, *119*, 12934–12939. (b) Blackmond, D. G. Kinetic Implications of Nonlinear Effects in Asymmetric Synthesis. *J. Am. Chem. Soc.* **1998**, *120*, 13349–13353. (c) Blackmond, D. G. Nonlinear Effects in Asymmetric Catalysis: Implications for Synthetic Strategies. In *Catalysis of Organic Reactions*; Herkes, F., Ed.; Marcel Dekker: New York, 1998; pp 455–465. (d) Blackmond, D. G.; Rosner, T.; Neugebauer, T.; Reetz, M. T. Kinetic Influences on Enantioselectivity for Non-Diastereopure Catalyst Mixtures. *Angew. Chem.* **1999**, *111*, 2333–2335; *Angew. Chem., Int. Ed.* **1999**, *38*, 2196–2199.
- (a) Noyori, R.; Kitamura, M. Enantioselective Addition of Organometallic Reagents to Carbonyl Compounds—Chirality Transfer, Multiplication, and Amplification. *Angew. Chem., Int. Ed. Engl.* **1991**, *30*, 49. (b) Kitamura, M.; Suga, S.; Oka, H.; Noyori, R. *J. Am. Chem. Soc.* **1998**, *120*, 9800.
- Noyori's more recent treatment (ref 8b), discussed in a later section of the paper, shows that the complexity of this system precludes complete analysis using the ML<sub>2</sub> model.
- Practical exploitation of asymmetric amplification may involve cases where the removal of a small impurity of the opposite ligand is difficult or uneconomical. See, for example, the section on stoichiometric asymmetric synthesis and the work of ref 23.
- The choice between an asymmetric and an achiral catalytic route often hinges on the question of productivity vs selectivity. Halpern has pointed out for the case of Rh<sup>+</sup>-catalyzed hydrogenation of enamides that reaction rates are much faster when the achiral DIPHOS ligand is used compared to enantiopure asymmetric ligands such as CHIRAPHOS or DIPAMP, and he has suggested that selectivity at the price of activity is an inevitable feature of these asymmetric catalytic reactions. Halpern, J. *Asymmetric Catalytic Hydrogenation: Mechanism and Origin of Enantioselection*. In *Asymmetric Synthesis, Vol. 5: Chiral Catalysis*; Morrison, J. D., Ed.; Academic Press, New York, 1985; Chapter 2, pp 41–69.
- The development of the models in this section is published here for the first time.
- (a) Girard, C.; Kagan, H. B. Nonlinear Effect in the Reduction of Acetophenone by Diisopinocampheyl Chloroborane: Influence of the Reagent Preparation. *Tetrahedron: Asymmetry* **1995**, *6*, 1881–1884. (b) Mikami, K.; Motoyama, Y.; Terada, M. Asymmetric Catalysis of Diels–Alder Cycloadditions by an MS-Free Binaphthol-Titanium Complex—Dramatic Effect of MS, Linear vs Positive Nonlinear Relationship, and Synthetic Applications. *J. Am. Chem. Soc.* **1994**, *116*, 2812–2820.
- Oguni, N.; Matsuda, Y.; Kaneko, T. Asymmetric Amplifying Phenomena in Enantioselective Addition of Diethylzinc to Benzaldehyde. *J. Am. Chem. Soc.* **1988**, *110*, 7877–7888.
- A model similar to that described in ref 8b was recently published: (a) Gutman, I. A Simple Model for Chiral Amplification in the Aminoalcohol-Catalyzed Reaction of Aldehydes with Dialkylzinc. *J. Serb. Chem. Soc.* **1999**, *64*, 447–452. (b) Gutman, I. A Note on the Noyori Model for Chiral Amplification in the Aminoalcohol-Catalyzed Reaction of Aldehydes with Dialkylzinc. *J. Serb. Chem. Soc.* **1999**, *64*, 681–684.
- (a) Mikami, K.; Terada, M. Chiral Titanium Complex-Catalyzed Carbonyl-Ene Reaction with Glyoxylate: Remarkable Positive Nonlinear Effect. *Tetrahedron* **1992**, *48*, 5671–5680. (b) Terada, M.; Matsumoto, Y.; Nakamura, Y.; Mikami, K. Molecular Assembly of BINOL-Ti Complexes into an Active  $\mu_3$ -oxo Titanium Catalyst. *Inorg. Chim. Acta* **1999**, *296*, 267–272. In this recent paper the authors also suggest that the trimer itself may be the active catalyst.
- A 6-fold and a 3-fold suppression reaction rate using a racemic mixture compared to the enantiopure catalyst are predicted for the irreversible and reversible models, respectively.
- de Vries, A. H. M.; Jansen, J. F. G. A.; Feringa, B. L. Enantioselective Conjugate Addition of Diethylzinc to Chalcones Catalysed by Chiral Ni(II) Aminoalcohol Complexes. *Tetrahedron* **1994**, *50*, 4479–4491.
- Bolm, C.; Ewald, M.; Felder, M. Catalytic Enantioselective Conjugate Addition of Dialkylzinc Compounds to Chalcones. *Chem. Ber.* **1992**, *125*, 1205–1215.
- “Incremental” enantioselectivity is the ee<sub>prod</sub> at a given instant in the reaction, in the absence of the reaction's prior history, and may be calculated from successive cumulative values.
- Bolm and co-workers (ref 19) eliminated this possibility after obtaining a similar ee<sub>prod</sub> in experiments where substrate was added during reaction. However, the substrate conversion level used for comparison was lower (ca. 40%) than that at which Figures 8 and 9 suggest that substrate effects become significant.
- Chandrasekharan, J.; Ramachandran, P. V.; Brown, H. C. Diisopinocampheylchloroborane, a Remarkably Efficient Chiral Reducing Agent for Aromatic Prochiral Ketones. *J. Org. Chem.* **1985**, *50*, 5446–5448.
- Zhao, M.; King, A. O.; Larsen, R. D.; Verhoeven, T. R.; Reider, R. J. A Convenient and Economical Method for the Preparation of DIP-Chloride<sup>TM</sup> and Its Application in the Asymmetric Reduction of Aralkyl Ketones. *Tetrahedron Lett.* **1997**, *38*, 2641–2644.
- Nonlinear effects in systems where the reaction products are enantiomeric but the catalysts are diastereomers or pseudo-diastereomers were first studied by Kagan and co-workers: Zhang, S. Y.; Girard, C.; Kagan, H. B. Nonlinear Effects Involving Two Competing Pseudo-Enantiomeric Catalysts: Example in Asymmetric Dihydroxylation of Olefins. *Tetrahedron: Asymmetry* **1995**, *6*, 2637–2640.
- Reetz, M. T.; Neugebauer, T. New Diphosphite Ligands for Catalytic Asymmetric Hydrogenation: The Crucial Role of Conformationally Enantiomeric Diols. *Angew. Chem.* **1999**, *111*, 134; *Angew. Chem., Int. Ed.* **1999**, *38*, 179.
- Bolm, C.; Muniz, K.; Hildebrand, J. P. Planar-Chiral Ferrocenes in Asymmetric Catalysis: The Impact of Stereochemically Inhomogeneous Ligands. *Org. Lett.* **1999**, *1*, 491–494.

AR990083S